ACS Chemical Neuroscience

Research Article

pubs.acs.org/chemneuro

Benzothiazepine CGP37157 Analogues Exert Cytoprotection in Various in Vitro Models of Neurodegeneration

Francisco J. Martínez-Sanz,[†,‡] Rocío Lajarín-Cuesta,[†] Ana J. Moreno-Ortega,[†,‡] Laura González-Lafuente,[†,‡] Jose C. Fernández-Morales,[†,§] Raquel López-Arribas,[†] María F. Cano-Abad,[*,†,‡] and Cristóbal de los Ríos[*,†,‡]

[†]Instituto Teófilo Hernando and Departamento de Farmacología y Terapéutica, Facultad de Medicina, Universidad Autónoma de Madrid, C/Arzobispo Morcillo, 4, 28029 Madrid, Spain

[‡]Servicio de Farmacología Clínica, Instituto de Investigación Sanitaria, Hospital Universitario de la Princesa, C/Diego de León, 62, 28006 Madrid, Spain

S *Supporting Information*

ABSTRACT: Mitochondria regulate cellular Ca^{2+} oscillations, taking up Ca^{2+} through its uniporter and releasing it through the mitochondrial sodium/calcium exchanger. The role of mitochondria in the regulation of Ca^{2+} cycle has received much attention recently, as it is a central stage in neuronal survival and death processes. Over the last decades, the 4,1-benzothiazepine CGP37157 has been the only available blocker of the mitochondrial sodium/calcium exchanger, although it targets several other calcium transporters. We report the synthesis of 4,1-benzothiazepine derivatives with the goal of enhancing mitochondrial sodium/calcium exchanger blockade and selectivity, and the evaluation of their cytoprotective effect. The compound **4c** presented an interesting neuroprotective profile in addition to an important blockade of the mitochondrial sodium/calcium exchanger. The use of this benzothiazepine could help to understand the physiological functions of the mitochondrial sodium/calcium exchanger. In addition, we hypothesize that a moderate blockade of the mitochondrial sodium/calcium exchanger would provide enhanced neuroprotection in neurons.

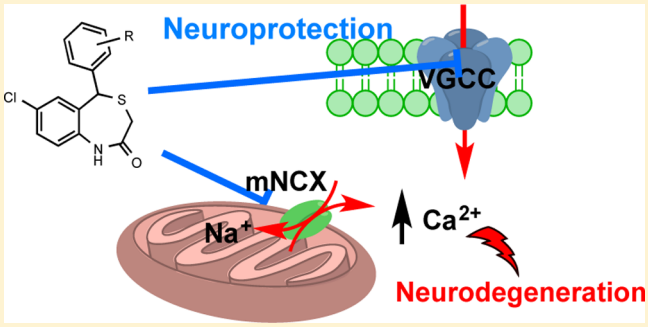

KEYWORDS: *Benzothiazepines, mitochondria, mNCX, NCLX, neurodegeneration, neuroprotection*

Besides their function as energy supplier, mitochondria play a central role in the regulation and handling of Ca^{2+} ions by cells.[1] Mitochondria redistribute cytosolic Ca^{2+} after its entry through calcium channels or its release from endoplasmic reticulum (ER), generating highly concentrated microdomains of Ca^{2+}, necessary for cellular functions, but avoiding a fatal Ca^{2+} overload.[2] The existence of a spatial colocalization between mitochondria, ER, and voltage-gated calcium channels (VGCC)[2] allows mitochondria to detect Ca^{2+} hot spots near both ER and VGCC, favoring the mitochondria-controlled Ca^{2+} redistribution. For this role, mitochondria uptake Ca^{2+} through its calcium uniporter,[3] and release it back to cytosol through H^+- and Na^+-coupled exchangers, being the sodium/calcium exchanger (mNCX) activity predominant in excitable cells.[4] Mitochondria are unable to store Ca^{2+}, since a sustained and elevated mitochondrial Ca^{2+} concentration ($[Ca^{2+}]_m$) induces the opening of the mitochondrial permeability transition pore and the subsequent activation of the apoptotic cascade.[5] Hence, the mNCX controls $[Ca^{2+}]_m$ and the Ca^{2+} crosstalk among mitochondria, cytosol, and ER.[6] Although the existence of the mNCX was hypothesized since the 1970s,[1] the protein was not discovered until 2010, which was named Na^+/Ca^{2+} or Li^+/Ca^{2+} exchanger (NCLX).[4,7] It belongs to the sodium/calcium exchangers superfamily, with which it shares similar structural motifs, but presenting the unique ability to transport Li^+ in exchange of Ca^{2+}, suggesting a different mechanism of ion selectivity.[8] Therefore, NCLX is the protein exclusively in charge of the sodium/calcium exchange at mitochondria, the "long-sought" mNCX.[4]

In the last decades, there have been few contributions discussing the synthesis of mNCX ligands,[9] although its dysfunction has been implicated in several pathologies such as diabetes[10] or neurodegenerative diseases.[11] As a consequence, pharmacological tools to study mNCX physiology are rather the same as in the 1980s.[12] The compound 7-chloro-5-(2′-chlorophenyl)-3,5-dihydro-4,1-benzothiazepin-2-(1*H*)-one (**1**; best-known as CGP37157; Figure 1) showed 20-fold higher blocking activity than the previously studied ligands,[13] and it remains as the reference ligand to study the mNCX.

Received: June 9, 2015
Revised: July 17, 2015
Published: July 20, 2015

DOI: 10.1021/acschemneuro.5b00161
ACS Chem. Neurosci. 2015, 6, 1626−1636

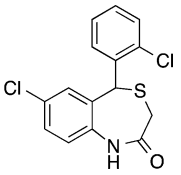

Figure 1. Chemical structure of CGP37157 (**1**).

This 4,1-benzothiazepine also blocks VGCC,[14,15] the plasmalemmal sodium/calcium exchanger,[16] and voltage-gated sodium channels[17] at similar concentrations. Attempts to find analogues with higher selectivity and improved mNCX blocking activity have been unsuccessful.[9] Some analogues of **1** were synthesized and their blockade evaluated in a pancreatic β-cell line, for their use in type II Diabetes Mellitus, although they were unable to improve the blockade exerted by **1**.[9] Indeed, 1,4-(or 4,1)-benzothiazepines have received much less attention than the 1,5-benzothiazepines, which are well-known VGCC blockers.[18,19] This issue has hindered the study of the role of mNCX in many physiological processes, and the question of whether blocking or enhancing mNCX activity could have a positive effect on different pathological processes.[11]

Deregulation of the intracellular $[Ca^{2+}]$ is a common event occurring in all neurodegenerative diseases.[20] In Alzheimer's disease (AD), there is an increased activity of Ca^{2+}-dependent protease enzymes in neurons containing neurofibrillary tangles.[21] Moreover, amyloid beta (Aβ) peptides increase the basal concentration of Ca^{2+}, sensitizing neurons to excitotoxicity and apoptosis.[22] In Parkinson's disease, α-synuclein aggregates can form ionic pores where Ca^{2+} can enter to neurons.[23] Also, mutations in protein deglycase-1, a rare type of familiar Parkinson's disease, produce alterations in Ca^{2+} homeostasis in knockout mice.[24] Amyotrophic lateral sclerosis (ALS) is another type of neurodegenerative disease where the Ca^{2+} homeostasis is compromised, in which a high exposure to the excitatory neurotransmitter glutamate is observed, which induces a high Ca^{2+} uptake,[25] contributing to the neuronal damage. PolyGln-expressing Huntingtin (Htt^{exp}), characteristic of Huntington's disease, alters Ca^{2+} concentrations in several critical points; Htt^{exp} binds inositol-1,4,5-triphosphate receptors, favoring the Ca^{2+} efflux from ER to cytosol,[26] and interacts with the NR2B subunit of the *N*-methyl-D-aspartate (NMDA) receptor, inducing an increase in Ca^{2+} inward currents.[27] These are a few examples of the huge amount of observations that correlate deregulation of Ca^{2+} homeostasis and neurodegenerative diseases.

It is important to highlight that NMDA receptors, which possess a Ca^{2+}-permeable ion channel, is a therapeutic target in AD and ALS, as proved by the fact that its blockers memantine and riluzole are prescribed for the treatment of such diseases,[28,29] although their efficacies are far from being satisfactory. VGCC blockers have also been studied for AD treatment, though they failed in clinic trials. By contrast, selective $Ca_v1.3$ blockers are being studied for the treatment of Parkinson disease with promising results.[30]

These findings give rise to the hypothesis whether the pharmacological intervention on the mitochondria-controlled regulation of intracellular Ca^{2+} has a therapeutic interest for the treatment of neurodegenerative diseases. In order to address this question, more potent and selective mNCX ligands should be developed and their neuroprotective activity proved in in vitro models of neurodegeneration. The discovery of such ligands would become a breakthrough in the study of the role of mNCX in neurodegeneration.

The neuroprotective profile of **1** against the Ca^{2+} overload-evoked cell death has been reported.[17] However, it remains unclear whether such neuroprotection was due to its ability to block the mNCX or due to interactions with other biological targets. For instance, we have also described that compound **1** is the first organic ligand that blocks the newly described Ca^{2+} channel CALHM1 (Ca^{2+} homeostasis modulator 1)[31] at submicromolar concentrations, in contrast to other 4,1-benzothiazepine analogues synthesized by our research group, which did not block CALHM1 so efficiently as **1**.[32] For these reasons, we decided to synthesize more derivatives of **1** with the goal of enhancing both mNCX blockade and selectivity, and assessing how such blockade could contribute to their neuroprotective profile. Our results indicate that improving the mNCX blockade would not be damaging neurons and, in turns, it would be protecting them in a scenario of neurodegeneration.

RESULTS AND DISCUSSION

Chemistry. Since the tridimensional structure of mNCX remains unknown, we proposed the design of **1** derivatives under classical strategies of pharmacodynamic modulation, replacing substituents at the anchored phenyl ring. These changes are aimed at the possible generation of new hydrogen bonds, increasing or reducing the steric volume, or shifting substituents from *ortho* to other positions, following experimental procedures previously described,[9] with slight modifications. Few other examples reporting syntheses of 4,1-benzothiazepines are found.[18,19] Boc-protected *para*-chloroaniline **2**[33] was subjected to *ortho*-lithiation conditions, and the addition of the corresponding aromatic aldehyde led to the formation of **3**. In the next step, by using neat trifluoroacetic acid (TFA), 4,1-benzothiazepine derivatives **4a–i** and **1** were obtained in a one-pot process (Scheme 1).

Scheme 1. Synthesis of Benzothiazepines 4a–j and 1[a]

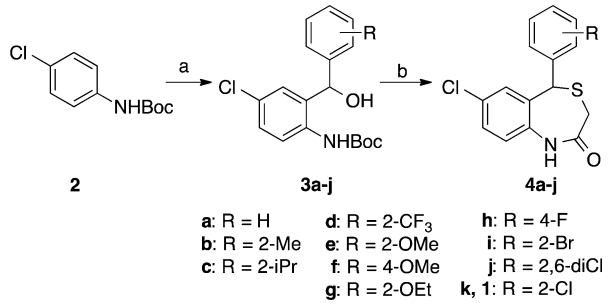

[a]Reagents and conditions: (a) (i) ^{t}BuLi, THF, −78 °C to −20 °C, 2 h; (ii) ArCHO, THF, −78 °C, 2 h; (b) methyl thioglycolate, TFA, 80 °C, 24 h.

Cytoprotection Experiments. These experiments were performed to evaluate the neuroprotective profile of the synthesized benzothiazepine derivatives in in vitro models of oxidative stress and Ca^{2+} overload-induced neurodegeneration, scenarios commonly found in neurodegenerative diseases. Veratridine causes both Na^+ and Ca^{2+} overload by delay in the inactivation of sodium channels,[34] increasing Na^+ entry, what drives to the cell depolarization and VGCC opening. We first assessed whether these **1** derivatives maintained that

DOI: 10.1021/acschemneuro.5b00161
ACS Chem. Neurosci. 2015, 6, 1626–1636

neuroprotective profile, measuring the release of lactate dehydrogenase (LDH), by a protocol previously described (Figure 2, Supporting Information Table S1).[14] In these

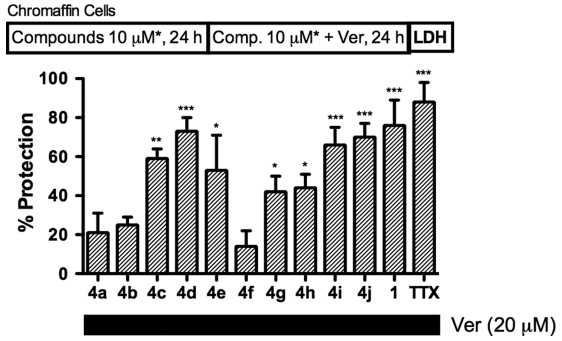

Figure 2. Effect of 4,1-benzothiazepines **4a–j** and **1** on the cell death, measured as LDH release, of bovine chromaffin cells subjected to veratridine (Ver) 20 μM. %Protection respect to the death observed in control cells in the absence of compounds. Data are expressed as means ± SEM of at least four different cell cultures in triplicate. *Compounds **4a** and **4f**, which precipitated in the assay media at 10 μM, were tested at 5 μM. *$p < 0.05$, **$p < 0.01$, and ***$p < 0.001$, with respect to control in the absence of compounds.

experiments, the sodium channel blocker tetrodotoxin (TTX) at 1 μM was used as a reference neuroprotectant against the veratridine-evoked cell death.[17]

Compounds **4a–j** were not as good as **1** in protecting bovine chromaffin cells from the damage evoked by veratridine, but most of them mitigated cell death in a statistically significant manner. Derivatives **4d**, **4i**, and **4j** presented a cytoprotective profile comparable to **1**. The presence of a bulky, preferentially halogenated, group at C2′ of the pending phenyl ring seems to be important to reduce the veratridine-induced cell death. We hypothesize that halogen atoms at the pending phenyl improve affinity of this kind of 4,1-benzothiazepines for sodium channels, as what was described for **1**.[17]

Another Ca^{2+} overload model of neurodegeneration where **1** had shown protective activity was that elicited by a high extracellular K^+ concentration.[17] For this reason, we compared the effect of **1** with its analogues **4a–j** in SH-SY5Y cells stimulated with K^+ 70 mM, measuring the loss of cell viability by the method of the MTT [(3-(4,5-dimethylthiazol-2-yl)-2,5-diphenyltetrazolium bromide] reduction (Figure 3, Table S2).[35] The VGCC blocker nifedipine (Nife) at 3 μM was included in the experiments as a reference neuroprotectant.[36]

In these experiments, five compounds (**4a**, **4c**, **4d**, **4i**, and **4j**) presented similar or higher protection than **1**. Again, we noticed a better protection when benzothiazepines bear a bulky group at C2′. But, similarly to the experiments with veratridine, derivatives having alkoxy substituents (**4e**, **4f**, and **4g**) do not provide neuroprotection. The loss of neuroprotection found with **4b** (R = 2-Me) is striking, taking into account the good activity of isosteric analogues **1** and **4d**. The incorporation of an additional chlorine atom at C6′ in compound **4j** (R_1 = 2-Cl, R_2 = 6-Cl) afforded equal protection than monosubstituted compound **1**.

However, from the point of view of neurodegenerative diseases, the most related model of Ca^{2+} overload-dependent neuronal death is that mediated by glutamate receptors.[37] In addition, the glutamate-elicited excitotoxicity has been proposed to be regulated by the mitochondria bioenergetics.[38]

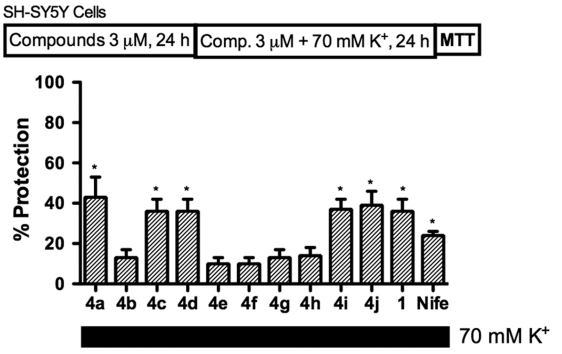

Figure 3. Effect of 4,1-benzothiazepines **4a–j** and **1** on the cell viability, measured as MTT reduction, of SH-SY5Y human neuroblastoma cells subjected to 70 mM K^+. %Protection respect to the loss of cell viability observed in control cells in the absence of compounds. Data are expressed as means ± SEM of at least four different cell batches in triplicate. *$p < 0.05$, with respect to control in the absence of compounds.

Taking into account these antecedents, we considered of interest testing these **1** analogues against the excitotoxicity elicited by glutamate. For this purpose, we used rat hippocampal slices exposed to glutamate 1 mM for 4 h, and the NMDA channels blocker memantine (Mem) was used as a reference neuroprotectant (Figure 4, Table S3).[14] Several

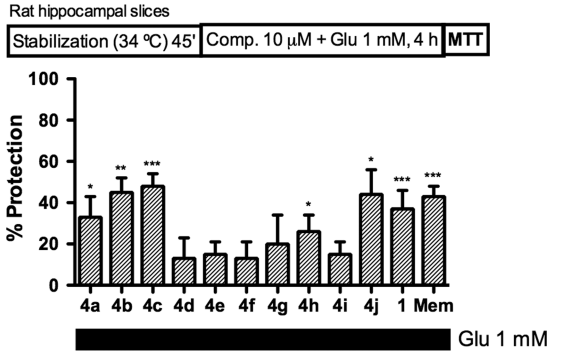

Figure 4. Effect of 4,1-benzothiazepines **4a–j** and **1** on the cell viability, measured as MTT reduction, of rat hippocampal slices subjected to glutamate (Glu) 1 mM. %Protection respect to the loss of cell viability observed in control slices in the absence of compounds. Data are expressed as means ± SEM of at least four different cell cultures in triplicate. ***$p < 0.001$, **$p < 0.01$, and *$p < 0.05$, with respect to control in the absence of compounds.

analogues protected hippocampal slices by 30% or more, highlighting compounds **4b** and **4c**, as they improved the neuroprotective activity observed with **1**. Compound **4j** showed a decent neuroprotection, but with low statistical significance. It seems that alkyl substituents at C2′ of the pending phenyl ring favor the ability to mitigate the damage exerted by glutamate. Again, alkoxy groups (present in **4e**, **4f**, and **4g** derivatives) reduced the neuroprotective profile. Chlorine atoms, present in compounds **1** and **4j** afford optimal neuroprotection against the glutamate exposure, unlike other halogens, present in derivatives **4d**, **4h**, and **4i**, which did not counteract the damage induced by glutamate (Figure 4).

A plethora of contributions have related increased oxidative stress in central nervous system to the progression of neurodegeneration and other pathologies,[39,40] where mitochondria play a pivotal role, due to generation of reactive oxygen

DOI: 10.1021/acschemneuro.5b00161
ACS Chem. Neurosci. 2015, 6, 1626–1636

species, as a consequence of its bioenergetic role. In this context, compound **1** lacked protective properties against the cell death induced by the cocktail of 10 μM oligomycin A and 30 μM rotenone (R/O), which blocks electron transport chain complexes V and I, respectively.[17] The R/O cocktail is a reproducible model of mitochondria-addressed oxidative stress, as electron transport chain disruption causes generation of free radicals and the reduction of the synthesis of ATP.[41] In a previous work, the isosteric analogue of **1**, **4b**, reduced the loss of neuronal viability elicited by R/O in SH-SY5Y neuroblastoma cells, with a maximal protection at 0.3 μM.[14] This observation prompted us to further evaluate the synthesized compounds in this model of oxidative stress (Figure 5, Table S4). Melatonin (Mel) at 30 nM was used as reference neuroprotective compound.[42]

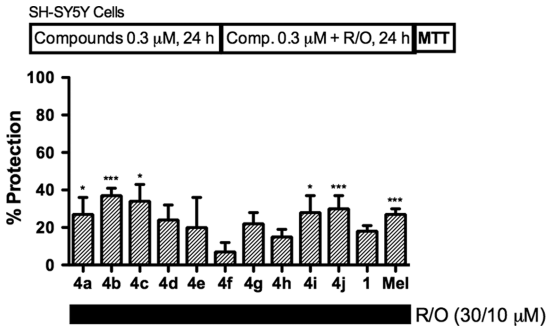

Figure 5. Effect of 4,1-benzothiazepines **4a–j** and **1** on the cell viability, measured as MTT reduction, of SH-SY5Y human neuroblastoma cells subjected to the stressor cocktail rotenone 30 μM and oligomycin A 10 μM (R/O). %Protection respect to the loss of cell viability observed in control cells in the absence of compounds. Data are expressed as means ± SEM of at least three different cell batches in triplicate. ***$p < 0.001$ and *$p < 0.05$, with respect to control in the absence of compounds.

Most of the compounds improved the neuroprotective profile evoked by **1** against the R/O cocktail, highlighting compounds **4b** and **4c**, which protected neuroblastoma cells by more than 30%. This antioxidant behavior is an additional property that the head compound **1** lacks. Again, bulky, alkyl-type groups at C2′ favor such activity. Besides, it is important to note that the unsubstituted derivative **4a** presented a slight neuroprotective behavior, similar to its activities represented in Figures 3 and 4. It seems that an unsubstituted phenyl ring is preferred to the existence of alkoxy groups to achieve neuroprotection. In summary, we have found five compounds with highlighted neuroprotection profile. Compounds **4a** (R = H), **4i** (R = 2-Br), and **4j** (R_1 = 2-Cl, R_2 = 6-Cl) surpassed **1** when counteracting the damage produced in SH-SY5Y cells by K^+ or R/O; compounds **4b** (R = 2-CH_3) and **4c** (R = 2-^{i}Pr) outdid **1** in neuroprotection experiments using glutamate or R/O as toxic stimuli; and compound **4d** (R = 2-CF_3) behaved as a good protectant when cells were subjected to both veratridine and high K^+ exposure. Overall, the most highlighted compound is **4c**, as it showed neuroprotection in all the in vitro models of neurodegeneration.

Evaluation of the mNCX Blockade by Compounds 1 and 4a–j. The burning question was whether the improvement in neuroprotection by some of the compounds was due, at least in part, to a better mNCX blockade. Thus, to test the ability of the new derivatives to regulate mitochondrial Ca^{2+} efflux through mNCX, we have carried out two different experimental procedures. In the first set of experiments, suitable for screening a huge battery of compounds, we stimulated HeLa cells with histamine. Histamine interacts with its plasmalemmal histamine receptors, which induces the synthesis of IP_3, that binds its receptor at the ER, triggering the Ca^{2+} release from ER, and this Ca^{2+} is rapidly taken up by mitochondria, as both organelles are closely coupled.[43] This histamine-induced mitochondrial Ca^{2+} increase and its posterior efflux to cytosol can be monitored with the mitochondria-targeted bioluminescent, Ca^{2+}-sensitive probe aequorin. The presence of mNCX blockers along the experiment will modify both shape and intensity of such $[Ca^{2+}]_m$ responses. Such is the case of **1**, which caused a prolonged increase of $[Ca^{2+}]_m$ in HeLa cells stimulated with histamine.[44] The use of HeLa cells is a reliable model to measure mNCX blocking activities, as they do not express VGCC or plasmalemmal NCX, the other major biological targets of benzothiazepine derivatives, so we can dissect the pharmacological activity carried out by derivatives **4a–j** and **1** on mNCX. We selected the concentration of 3 μM to test all the compounds, based on concentration–response experiments performed with **1** (Figure S1). The kinetic parameters studied in the registers of $[Ca^{2+}]_m$ were the clearance constant, defined as the decay rate (τ_{off}), the uptake constant, defined as the rise rate (τ_{on}), the area under the curve (AUC), and the peak (i.e., maximal peak of $[Ca^{2+}]_m$ reached) (Figure S2). Only compound **4c** augmented AUC in a statistically significant fashion (Figure 6A). Like **4c**, unsubstituted derivative **4a** elevated $[Ca^{2+}]_m$ peak compared with the control situation, with statistical significance (Figure 6B). As far as the rise rate, that is, τ_{on}, compounds **4g** and **4h** accelerated the Ca^{2+} influx by mitochondria (Figure 6C). Finally, the analysis of the clearance constant as decay time, that is, τ_{off}, showed that, similarly to what was found with compound **1**, compounds **4a**, **4c**, **4e**, **4g**, and **4i** slowed down the mitochondrial Ca^{2+} efflux to the cytosol (Figure 6D).

Altogether, we have found several derivatives that improve the mNCX blocking activity of **1**, with compounds **4a** and **4c** standing out. Such compounds would maintain higher concentration of Ca^{2+} inside the mitochondria, and during more time, what could help to avoid fatal high Ca^{2+} elevations in the cytosol. As far as the relationship between mNCX blockade and neuroprotection, such a hypothesis is fulfilled for compounds **4a**, **4c**, and **4i**, based on the improvement that they show in mNCX blockade and neuroprotection, and for **4f**, due to the absence of neuroprotective properties neither mNCX blockade. By contrast, **4b**, **4d**, and **4j** showed neuroprotection in some in vitro models of neurodegeneration, but lacked effect on mNCX, suggesting the possibility that another biological target could be implicated. Compounds **4e** and **4g** presented weak neuroprotective activities along with a weak mNCX blockade.

Gathering all of these values, compound **4c** proved to be the most promising candidate to evaluate its mNCX blocking activity in a more sophisticated type of experiments, using permeabilized cells, affording a direct evidence of mNCX blockade, using specific experimental conditions that induce Ca^{2+} uptake by mitochondria and its subsequent efflux back to cytosol, where potential mNCX blockers will change the shape and amplitude of the mitochondrial Ca^{2+} oscillations. Ca^{2+} uptake by mitochondria was induced with an intracellular solution containing 5 μM Ca^{2+}, and its outflow to cytosol was

DOI: 10.1021/acschemneuro.5b00161
ACS Chem. Neurosci. 2015, 6, 1626–1636

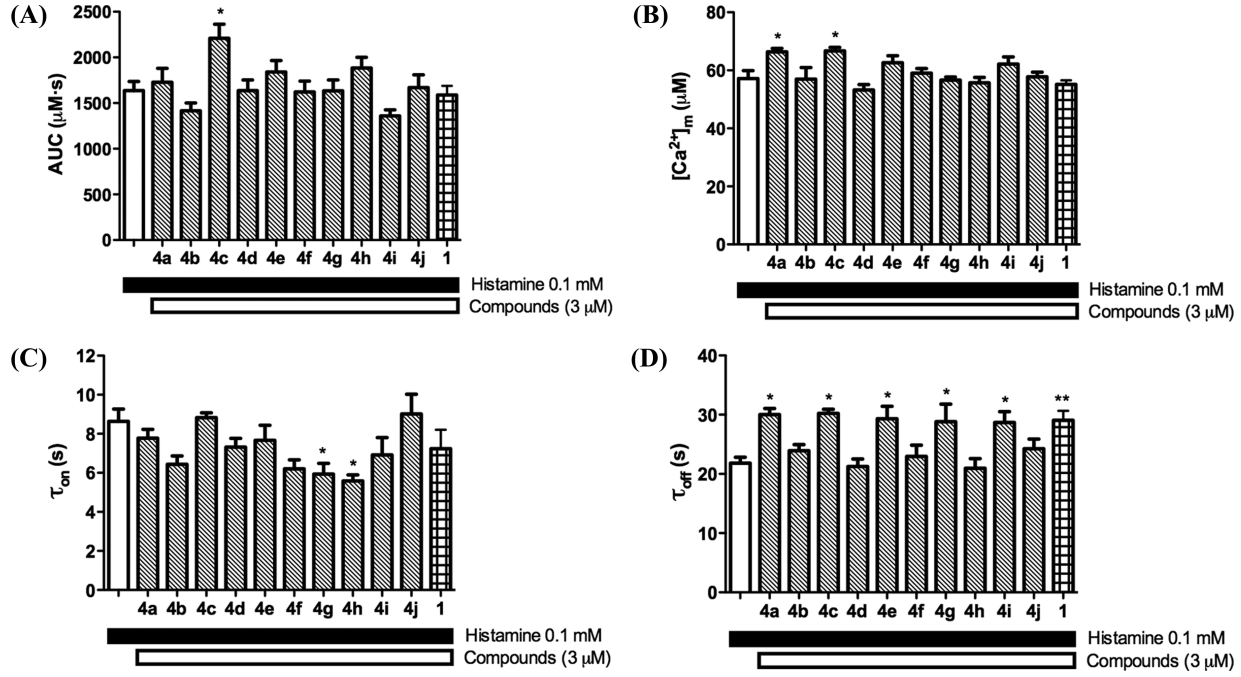

Figure 6. Effects of **1** and its derivatives **4a–j** on the histamine-induced mitochondrial $[Ca^{2+}]$ ($[Ca^{2+}]_m$) oscillations in HeLa cells, measured with the mitochondrial aequorin. Panels (A) and (B) show AUC and mean of peak increases, respectively, of the $[Ca^{2+}]_m$ elevations. Panels (C) and (D) show rise and decay rates, respectively, of the $[Ca^{2+}]_m$ elevations. Mean of at least nine experiments with cells from three different cultures. Data are expressed as mean ± SEM. *$p < 0.05$ and **$p < 0.01$, with respect to control in the absence of compounds (white bars).

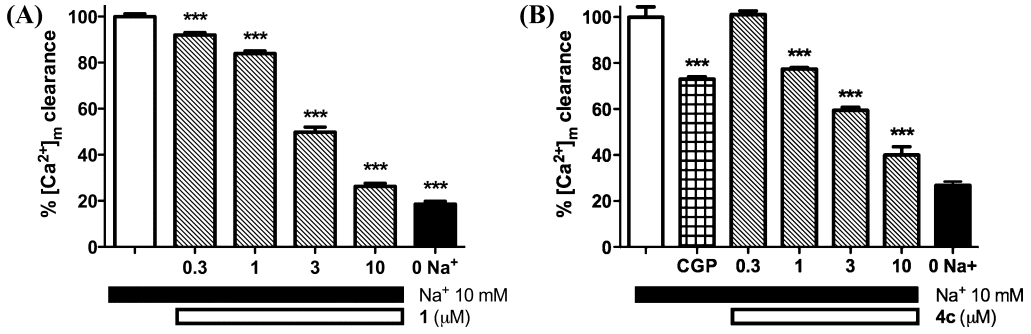

Figure 7. Effects on the 10 mM Na^+-stimulated $[Ca^{2+}]_m$ clearance in permeabilized HeLa cells by **1** (panel A) and **4c** (panel B), measured with mitochondrial-targeted aequorin. Ca^{2+} uptake by mitochondria was achieved by applying an intracellular solution with Ca^{2+} 5 μM, and its subsequent release was stimulated by an intracellular solution containing Na^+ 10 mM. Compound **1** at the concentration of 1.6 μM, which was the EC_{50} obtained in previous experiments, was used as a reference. Data are expressed as mean ± SEM of at least 10 experiments with cells from four different cultures. ***$p < 0.001$, with respect to the maximal mNCX activity in the absence of compounds (white bars).

induced by an intracellular solution containing 10 mM Na^+. In parallel, we confirmed that these selected compounds did not reduce the cell viability of HeLa cells (Figure S3) at similar concentrations to those used in these experiments. Figure 7 shows the $[Ca^{2+}]_m$ clearance constants in permeabilized HeLa cells stimulated with 10 mM Na^+, in the presence of increasing concentrations of the selected compounds incubated during the whole protocol. The maximal mNCX activity, defined as the positive control (Figure 7, white bars), was obtained in experiments in which the tested compounds were absent. In another batch of cells, where a 0 Na^+ solution was applied, mNCX was not able to buffer the increase of $[Ca^{2+}]_m$, thus defining the minimal mNCX activity (Figure 7, black bars). The tiny clearance of $[Ca^{2+}]_m$ observed in this particular situation is only ascribed to the activity of the mitochondrial Ca^{2+}/H^+ pump.

In these experiments, compound **1**, from 3 μM, promoted a significant reduction of the $[Ca^{2+}]_m$ clearance in a concentration-dependent reduction of the (Figure 7A). With these data, an EC_{50} of 1.6 μM was calculated, in concordance to what has been previously described.[9] On the other hand, compound **4c** induced a significant reduction of the $[Ca^{2+}]_m$ clearance from 1 μM (Figure 7B), also in a concentration-dependent manner, having an EC_{50} of 0.69 μM, being 2.3-fold lower than that observed for the classical mNCX blocker **1**. In parallel, compound **1** at the concentration reaching its EC_{50}, that is, 1.6 μM, was applied to HeLa cells, for comparative purposes, observing that $[Ca^{2+}]_m$ clearance was similar to the situation of applying **4c** at 1 μM (Figure 7B). The fact that the best neuroprotectant of the family also improved the mNCX blockade exerted by **1** would confirm our hypothesis, supported by the idea that a slight reduction of the mitochondrial Ca^{2+} release rate to cytosol could be beneficial to enhance the

DOI: 10.1021/acschemneuro.5b00161
ACS Chem. Neurosci. 2015, 6, 1626–1636

neuroprotective properties in a scenario of neuronal damage, as that found in neurodegenerative diseases. Mitochondrial Ca^{2+} needs to be finely regulated, as a high and sustained elevation of the $[Ca^{2+}]_m$ could trigger proapoptotic events, mainly by the generation of reactive oxygen species.[5] In our particular situation, where these benzothiazepine derivatives slow down the release of Ca^{2+} from mitochondria, the subsequent increase of $[Ca^{2+}]_m$ is far from generating neuronal damage. As we proved in experiments using DCFDA (2′,7′-dichlorofluorescin diacetate), a fluorogenic dye that measures hydroxyl, peroxy, and other reactive oxygen species (ROS) within the cell, the administration of **1** or the best blocker of the family **4c**, at a concentration close to their EC_{50} (1 μM), did not generate additional ROS compared to a basal situation, (Figure S4). The stressor cocktail R/O at concentrations of 30 μM for rotenone and 10 μM for oligomycin A, was used as standard of a typical ROS generation derived by mitochondrial damage.

As commented previously, the neuroprotective profile of **4b** and **4d** in neuronal models of Ca^{2+} overload (i.e., 70 mM K^+ and glutamate exposure) which has not been related to a mNCX blockade, could be associated with the interaction with another biological target. Therefore, taking into account the described VGCC blocking activity of **1**,[15] we wondered whether these two compounds would be also acting as Ca^{2+} antagonists. Moreover, we also evaluated whether the best mNCX blocker discovered of this 4,1-benzothiazepines family, **4c**, could be also blocking VGCC. To figure it out, patch-clamp experiments with the selected compounds were performed. We have recorded the modulation exerted by these derivatives on the whole-cell inward Ca^{2+} currents through VGCC (I_{Ca}), when bovine chromaffin cells were subjected to voltage depolarizing pulses, by patch-clamp in its perforated-patch configuration (Figure 8).

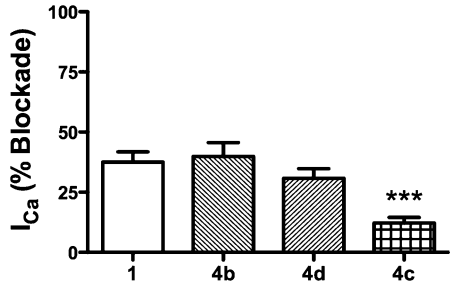

Figure 8. Partial blockade by **1** and **4b–d** of Ca^{2+} currents (I_{Ca}) stimulated by depolarization. Whole-cell I_{Ca} was monitored under perforated-patch mode, using 5 mM Ca^{2+} as charge carrier, with −80 mV as holding voltage. Averaged results showing of I_{Ca} blockades. ***$p < 0.001$, with respect to the blockade of **1** (white bar).

Compound **1** efficiently blocked I_{Ca} by 37% in bovine chromaffin cells at 10 μM (Figure 8). Similar blockades were found with **4b** and **4d**, which had presented a good neuroprotective profile, but lacking effect on mNCX. Hence, we can correlate their neuroprotective effect with such VGCC antagonist behavior. Compound **4c** showed a much lesser Ca^{2+} antagonist effect (12% of I_{Ca} reduction, Figure 8). In addition, compound **4c** did not affect Na^+ channels, as demonstrated by the fact that removal of the Na^+ channel blocker TTX from the tyrode solution did not derived in an additional blockade of currents (data not shown). Therefore, comparing these data with those from the experiments of mNCX blockade in permeable HeLa cells (Figure 7), it can be established that **4c** is much more selective to block mNCX (EC_{50} of 0.69 μM) than to block VGCC, compared with compound **1**.

CONCLUSIONS

We have found several compounds possessing a broad-spectrum neuroprotective profile. Such neuroprotection could not only be due to the mNCX blockade, as some of them, for example, **4b**, **4d**, and **4j**, did not affect the histamine-induced $[Ca^{2+}]_m$ increase (Figure 6). A possibility exists to ascribe their neuroprotective effect to the VGCC blocking activity, as pointed out by patch-clamp experiments (Figure 8). Indeed, L-type VGCCs are efficiently blocked by the closely related 1,5-benzothiazepines.[45] In the case of **4c**, its neuroprotection profile is not related to a VGCC blockade, as it only reduced I_{Ca} by 12% at 10 μM, but ascribed to its blocking activity of mNCX. It is important to note that, although **4c** did not block VGCC, it maintained the ability of **1** to protect against Ca^{2+} overload models, that is, exposure to 70 mM K^+, veratridine, or glutamate. This fact would support the hypothesis that mNCX is a valuable target to control Ca^{2+} homeostasis in situations of neurodegeneration, and the lack of activity on calcium channels would reduce the possibility to present peripheral cardiovascular adverse effects. But this selectivity is not only important in terms of absence of potential side effects. The new compound **4c** could be used as an improved pharmacological tool for the study of the role of mNCX in both physiological and pathological situations, where it had been implicated. These studies have always used **1** as a pharmacological tool, obtaining results that are, in some cases, contradictory.[46] The reason for such contradictions is undoubtedly derived by its blocking activity on biological targets like VGCC, plasmalemmal NCX, sodium channels, or CALHM1. We have recently reported that compound **4c** scarcely affects the Ca^{2+} uptake through CALHM1.[32] Hence, we propose **4c** (compound that we have named ITH12575) as a more potent and selective mNCX blocker than the best-known **1** (CGP37157). On top of that, **4c** mitigated the neuronal damage in a model of oxidative stress, a property that the head compound **1** did not showed. Therefore, our hypothesis regarded to the design of mNCX ligands for the development of new neuroprotective compounds, seems to be confirmed.

METHODS

General Procedures. Reagents and solvents were purchased from commercial providers (Sigma-Aldrich, Carlo-Erba, VWR). All the arylaldehydes were commercially available, except 2-isopropylbenzaldehyde, for the synthesis of **3c**.[32] Reactions were followed by thin layer chromatography, with precoated plates of silica gel. Detection was made with UV light at 254 nm. All the reactions were subjected to Schlenk conditions (vacuum purges and argon atmosphere). Removal of solvents was done with a rotary evaporator under vacuum. Precharged silica gel columns (230–400 mesh) were used in a Biotage chromatographic station. Melting points were determined in a Stuart apparatus (SMP-10) and are not corrected. MS spectra were obtained in a QSTAR de ABSciex apparatus. ^1H and ^{13}C NMR spectra were carried out with a Bruker AVANCE 300 MHz instrument, and measurements were carried out at 26 °C and described as ppm using deuterated solvents as internal standard. IR spectra were registered in an IFS66v spectrophotometer (Bruker). Compounds **4a–j** had a purity of 95% or more, measured by HPLC.

General Procedure for the Preparation of 4-Chloro-2-[hydroxy(aryl)methyl]-*N*-*tert*-butoxycarbonylanilines 3a–k. We followed an experimental procedure previously described,[9] with slight modifications. To a solution of 4-chloro-*N*-*tert*-butoxycarbonylaniline **2**[33] (1 equiv) in dry THF (15 mL), ^{t}BuLi (1.7 M in hexanes,

DOI: 10.1021/acschemneuro.5b00161
ACS Chem. Neurosci. 2015, 6, 1626–1636

2.7 equiv) was added dropwise at −78 °C under Ar, and the reaction was stirred at this temperature for 15 min, and then it was stirred for 2 h at −10 °C. After this time, reaction was cooled down to −78 °C, the corresponding arylaldehyde (1.1 equiv) in dry THF (5 mL) was added dropwise, and the reaction was stirred 2 h at this temperature. Reaction was terminated by addition of water (15 mL), and once it reached room temperature, it was extracted with diethyl ether (3 × 30 mL). Then, the combined organic layer was washed with brine (3 × 50 mL), dried with anhydrous $MgSO_4$, filtered, and concentrated, to obtain a yellow oil that was purified by flash chromatography in automatized flash chromatographer using ethyl acetate/hexane mixtures as eluent.

*4-Chloro-2-[hydroxy(phenyl)methyl]-N-tert-butoxycarbonylaniline (**3a**).* Following the general procedure for the preparation of 4-chloro-2-[hydroxy(aryl)methyl]-*N-tert*-butoxycarbonylanilines **3a**−**k**, reaction of **2** (100 mg, 0.44 mmol) with benzaldehyde (0.48 mmol, 51 mg) yielded **3a** (64 mg, 49%). ^{1}H NMR (300 MHz, $CDCl_3$) δ 7.78 (d, J = 8.6 Hz, 1H), 7.55 (s, 1H), 7.40−7.22 (m, 6H), 7.02 (d, 1H, J = 2.3 Hz), 5.85 (s, 1H), 2.89 (bs, 1H), 1.44 (s, 9H).

*4-Chloro-2-[hydroxy(o-toluyl)methyl]-N-tert-butoxycarbonylaniline (**3b**).* Following the general procedure for the preparation of 4-chloro-2-[hydroxy(aryl)methyl]-*N-tert*-butoxycarbonylanilines **3a**−**k**, reaction of **2** (500 mg, 2.20 mmol) with *o*-tolualdehyde (2.55 mmol, 358 mg) yielded **3b** (520 mg, 68%). ^{1}H NMR (300 MHz, $CDCl_3$) δ 7.79 (d, J = 8.7 Hz, 1H), 7.51−7.46 (m, 2H), 7.31−7.18 (m, 4H), 6.80 (d, J = 2.7 Hz, 1H), 6.03 (d, J = 3.9 Hz, 1H), 2.67 (d, J = 3.9 Hz, 1H), 1.51 (s, 9H).

*4-Chloro-2-[hydroxy(2′-isopropylphenyl)methyl]-N-tert-butoxycarbonylaniline (**3c**).* Following the general procedure for the preparation of 4-chloro-2-[hydroxy(aryl)methyl]-*N-tert*-butoxycarbonylanilines **3a**−**k**, reaction of **2** (100 mg, 0.44 mmol) with 2-isopropylbenzaldehyde (0.48 mmol, 72 mg) yielded **3c** (85 mg, 51%). ^{1}H NMR (300 MHz, $CDCl_3$) δ 7.80 (d, J = 8.6 Hz, 1H), 7.42 (s, 1H), 7.40−7.37 (m, 3H), 7.30−7.22 (m, 2H), 6.90 (d, J = 2.3 Hz, 1H), 6.15 (s, 1H), 3.05 (p, J = 6.8 Hz, 1H), 2.40 (bs, 1H), 1.55 (s, 9H), 1.28 (d, J = 6.8 Hz, 3H), 1.18 (d, J = 6.8 Hz, 3H). ^{13}C NMR (75.4 MHz, $CDCl_3$) δ 153.4, 146.7, 137.0, 135.4, 134.1, 128.9, 128.7, 128.5, 128.0, 126.7, 126.4, 126.2, 123.3, 80.8, 70.1, 28.6, 28.3, 24.2, 23.7.

*4-Chloro-2-[hydroxy(2′-trifluoromethylphenyl)methyl]-N-tert-butoxycarbonylaniline (**3d**).* Following the general procedure for the preparation of 4-chloro-2-[hydroxy(aryl)methyl]-*N-tert*-butoxycarbonylanilines **3a**−**k**, reaction of **2** (500 mg, 2.20 mmol) with 2-trifluoromethylbenzaldehyde (2.42 mmol, 421 mg) yielded **3d** (406 mg, 46%). ^{1}H NMR (300 MHz, $CDCl_3$) δ 7.72−7.61 (m, 4H), 7.47 (m, 1H), 7.24 (dd, J = 8.7, 2.7 Hz, 1H), 7.17 (s, 1H), 6.94 (d, J = 2.4 Hz, 1H), 6.29 (d, J = 3.0 Hz, 1H), 3.27 (d, J = 3.0 Hz, 1H), 1.48 (s, 9H).

*4-Chloro-2-[hydroxy(2′-methoxyphenyl)methyl]-N-tert-butoxycarbonylaniline (**3e**).* Following the general procedure for the preparation of 4-chloro-2-[hydroxy(aryl)methyl]-*N-tert*-butoxycarbonylanilines **3a**−**k**, reaction of **2** (500 mg, 2.20 mmol) with 2-methoxybenzaldehyde (2.42 mmol, 329 mg) yielded **3e** (291 mg, 36%). ^{1}H NMR (300 MHz, $CDCl_3$) δ 8.18 (s, 1H), 7.95 (d, J = 6.0 Hz), 7.40−7.29 (m, 3H), 7.08−6.97 (m, 3H), 6.16 (s, 1H), 3.92 (s, 3H), 2.85 (bs, 1H), 1.59 (s, 9H).

*4-Chloro-2-[hydroxy(4′-methoxyphenyl)methyl]-N-tert-butoxycarbonylaniline (**3f**).* Following the general procedure for the preparation of 4-chloro-2-[hydroxy(aryl)methyl]-*N-tert*-butoxycarbonylanilines **3a**−**k**, reaction of **2** (500 mg, 2.20 mmol) with 4-methoxybenzaldehyde (2.42 mmol, 329 mg) yielded **3f** (511 mg, 64%). ^{1}H NMR (300 MHz, $CDCl_3$) δ 7.81 (d, J = 8.6 Hz, 1H), 7.57 (bs, 1H), 7.25 (m, 3H), 7.02 (d, J = 2.7 Hz, 1H), 6.90 (m, 2H), 5.82 (s, 1H), 3.81 (s, 3H), 2.64 (bs, 1H), 1.45 (s, 9H).

*4-Chloro-2-[hydroxy(2′-ethoxyphenyl)methyl]-N-tert-butoxycarbonylaniline (**3g**).* Following the general procedure for the preparation of 4-chloro-2-[hydroxy(aryl)methyl]-*N-tert*-butoxycarbonylanilines **3a**−**k**, reaction of **2** (500 mg, 2.20 mmol) with 2-ethoxybenzaldehyde (2.42 mmol, 363 mg) yielded **3g** (463 mg, 56%). ^{1}H NMR (300 MHz, $CDCl_3$) δ 7.98 (bs, 1H), 7.89 (d, J = 8.6 Hz, 1H), 7.30−7.20 (m, 3H), 7.10 (d, J = 2.7 Hz, 1H), 6.95 (m, 2H), 6.10 (d, J = 6.0 Hz, 1H), 4.12 (c, J = 7.0 Hz, 2H), 3.45 (d, J = 6.0 Hz, 1H), 1.45 (s, 9H), 1.35 (t, J = 7.0 Hz, 3H).

*4-Chloro-2-[hydroxy(4′-fluorophenyl)methyl]-N-tert-butoxycarbonylaniline (**3h**).* Following the general procedure for the preparation of 4-chloro-2-[hydroxy(aryl)methyl]-*N-tert*-butoxycarbonylanilines **3a**−**k**, reaction of **2** (500 mg, 2.20 mmol) with 4-fluorobenzaldehyde (2.42 mmol, 300 mg) yielded **3h** (356 mg, 46%). ^{1}H NMR (300 MHz, $CDCl_3$) δ 7.76 (d, J = 8.7 Hz, 1H), 7.43 (bs, 1H), 7.32−7.23 (m, 3H), 7.07−7.01 (m, 3H), 5.84 (d, J = 3.3 Hz, 1H), 2.83 (d, J = 3.3 Hz, 1H), 1.43 (s, 9H).

*4-Chloro-2-[hydroxy(2′-bromophenyl)methyl]-N-tert-butoxycarbonylaniline (**3i**).* Following the general procedure for the preparation of 4-chloro-2-[hydroxy(aryl)methyl]-*N-tert*-butoxycarbonylanilines **3a**−**k**, reaction of **2** (500 mg, 2.20 mmol) with 2-bromobenzaldehyde (2.42 mmol, 447 mg) yielded **3i** (320 mg, 35%). ^{1}H NMR (300 MHz, $CDCl_3$) δ 7.65 (d, J = 8.7 Hz, 1H), 7.59−7.51 (m, 2H), 7.41(bs, 1H), 7.36 (m, 1H), 7.25−7.16 (m, 2H), 6.91 (d, J = 2.7 Hz, 1H), 6.10 (s, 1H), 3.78 (bs, 1H), 1.48 (s, 9H).

*4-Chloro-2-[hydroxy(2′,6′-dichlorophenyl)methyl]-N-tert-butoxycarbonylaniline (**3j**).* Following the general procedure for the preparation of 4-chloro-2-[hydroxy(aryl)methyl]-*N-tert*-butoxycarbonylanilines **3a**−**k**, reaction of **2** (500 mg, 2.20 mmol) with 2,6-dichlorobenzaldehyde (2.39 mmol, 418 mg) yielded **3j** (562 mg, 64%). ^{1}H NMR (300 MHz, $CDCl_3$) δ 8.23 (bs, 1H), 7.93 (d, 1H, J = 8.6 Hz), 7.29 (d, 1H, J = 8.6 Hz), 7.18−7.09 (m, 3H), 6.44 (m, 2H), 3.87 (bs, 1H), 1.40 (s, 9H).

*4-Chloro-2-[hydroxy(2′-chlorophenyl)methyl]-N-tert-butoxycarbonylaniline (**3k**).* Following the general procedure for the preparation of 4-chloro-2-[hydroxy(aryl)methyl]-*N-tert*-butoxycarbonylanilines **3a**−**k**, reaction of **2** (500 mg, 2.20 mmol) with 2-chlorobenzaldehyde (2.42 mmol, 340 mg) yielded **3k** (380 mg, 47%). ^{1}H NMR (300 MHz, $CDCl_3$) δ 7.69 (d, 1H, J = 8.6 Hz), 7.52 (d, 1H J = 8.6 Hz), 7.40−7.20 (m, 5H), 6.90 (d, 1H, J = 2.3 Hz), 6.15 (bs, 1H), 3.32 (bs, 1H), 1.45 (s, 9H).

General Procedure for the Preparation of 7-Chloro-5-aryl-3,5-dihydro-4,1-benzothiazepin-2-(1*H*)-ones 4a−j and 1. To a solution of methyl thioglycolate (3−6 equiv) in freshly distilled TFA (14 equiv), compound **3a**−**k** (1 equiv) was added. The reaction was stirred at 85 °C for 24 h. Then, it was dissolved in CH_2Cl_2 (30 mL) and washed with brine (30 mL), 1 N $NaOH_{aq}$ (30 mL), and brine (30 mL). The resulting organic layer was dried over Na_2SO_4, filtered, and concentrated, to obtain a crude that was further purified by automatized flash chromatography, using ethyl acetate/hexane mixtures as eluent, to give pure compounds with analytical and spectral data according with their structure.

*7-Chloro-5-phenyl-3,5-dihydro-4,1-benzothiazepin-2-(1H)-one (**4a**).* Following the general procedure for the preparation of 7-chloro-5-aryl-3,5-dihydro-4,1-benzothiazepin-2-(1*H*)-ones **4a**−**j** and **1**, reaction of **3a** (311 mg, 0.93 mmol) with methyl thioglycolate (2.79 mmol, 296 mg) in TFA (13.38 mmol, 1.53 g, 1.03 mL) yielded **4a** (174 mg, 65%) as a white solid, showing analytical and spectral data in accordance with the literature.[9]

*7-Chloro-5-(o-toluyl)-3,5-dihydro-4,1-benzothiazepin-2-(1H)-one (**4b**).* Following the general procedure for the preparation of 7-chloro-5-aryl-3,5-dihydro-4,1-benzothiazepin-2-(1*H*)-ones **4a**−**j** and **1**, reaction of **3b** (100 mg, 0.29 mmol) with methyl thioglycolate (0.88 mmol, 93 mg) in TFA (4.16 mmol, 474 mg, 320 μL) yielded **4b** (50 mg, 57%) as a white solid, showing analytical and spectral data in accordance with the literature.[9]

*7-Chloro-5-(2′-isopropylphenyl)-3,5-dihydro-4,1-benzothiazepin-2-(1H)-one (**4c**).* Following the general procedure for the preparation of 7-chloro-5-aryl-3,5-dihydro-4,1-benzothiazepin-2-(1*H*)-ones **4a**−**j** and **1**, reaction of **3c** (1.34 g, 3.57 mmol) with methyl thioglycolate (21.43 mmol, 2.27 g) in TFA (50.01 mmol, 5.70 g, 3.82 mL) yielded **4c** (859 mg, 73%) as a white solid, showing analytical and spectral data in accordance with the literature.[32]

*7-Chloro-5-(2′-trifluoromethylphenyl)-3,5-dihydro-4,1-benzothiazepin-2-(1H)-one (**4d**).* Following the general procedure for the preparation of 7-chloro-5-aryl-3,5-dihydro-4,1-benzothiazepin-2-(1*H*)-ones **4a**−**j** and **1**, reaction of **3d** (277 mg, 0.69 mmol) with methyl

DOI: 10.1021/acschemneuro.5b00161
ACS Chem. Neurosci. 2015, 6, 1626−1636

thioglycolate (5.66 mmol, 602 mg) in TFA (13.24 mmol, 1.51 g, 1.01 mL) yielded **4d** (182 mg, 74%) as a white solid. Mp 179−181 °C. ^{1}H NMR (300 MHz, $CDCl_3$) δ 8.08 (d, J = 8.1 Hz, 1H), 7.73 (m, 2H), 7.53 (m, 1H), 7.45 (bs, 1H), 7.25 (m, 1H), 7.05 (d, J = 8.5 Hz, 1H), 6.72 (d, J = 1.8 Hz, 1H), 6.17 (s, 1H), 3.40 (d, J = 12.1 Hz, 1H), 3.00 (d, J = 12.1 Hz, 1H). ^{13}C NMR (75.4 MHz, $CDCl_3$) δ 169.4, 136.0, 134.5, 134.4, 133.4, 132.3, 132.1, 129.0, 128.9, 127.9, 127.2 (c, J = 8.0 Hz), 125.4, 42.4, 31.7. Anal. Calcd for $C_{16}H_{11}ClF_3NOS$: C, 53.71; H, 3.10; N, 3.91. Found: C, 53.82; H, 3.17; N, 3.83.

*7-Chloro-5-(2′-methoxyphenyl)-3,5-dihydro-4,1-benzothiazepin-2-(1H)-one (**4e**).* Following the general procedure for the preparation of 7-chloro-5-aryl-3,5-dihydro-4,1-benzothiazepin-2-(1*H*)-ones **4a−j** and **1**, reaction of **3e** (100 mg, 0.27 mmol) with methyl thioglycolate (0.82 mmol, 87 mg) in TFA (3.96 mmol, 452 mg, 303 μL) yielded **4e** (53 mg, 60%) as a white solid. Mp 213-215 °C. ^{1}H NMR (300 MHz, $CDCl_3$) δ 7.72 (dd, J = 8.6, 1.6 Hz, 1H), 7.35 (m, 1H), 7.22 (m, 1H), 7.08 (m, 1H), 6.99 (m, 1H), 6.88 (m, 2H), 6.14 (s, 1H), 3.70 (s, 3H), 3.32 (d, J = 12.1 Hz, 1H), 3.00 (d, J = 12.1 Hz, 1H). ^{13}C NMR (75.4 MHz, $CDCl_3$) δ 170.1, 156.8, 136.9, 134.9, 134.2, 133.2, 130.6, 129.7, 128.4, 125.3, 124.5, 120.8, 111.1, 55.7, 40.0, 31.6. HRMS: m/z (M + H)$^+$ calcd. for $C_{16}H_{15}ClNO_2S$ 320.0512, found 320.0504.

*7-Chloro-5-(4′-methoxyphenyl)-3,5-dihydro-4,1-benzothiazepin-2-(1H)-one (**4f**).* Following the general procedure for the preparation of 7-chloro-5-aryl-3,5-dihydro-4,1-benzothiazepin-2-(1*H*)-ones **4a−j** and **1**, reaction of **3f** (115 mg, 0.32 mmol) with methyl thioglycolate (1.90 mmol, 202 mg) in TFA (4.40 mmol, 502 mg, 337 μL) yielded **4f** (56 mg, 56%) as a white solid. Mp 247−249 °C (decomp. 221 °C). ^{1}H NMR (300 MHz, $CDCl_3$) δ 7.51 (s, 1H), 7.40 (d, J = 8.5 Hz, 2H), 7.24 (m, 1H), 7.02 (d, J = 8.5 Hz, 1H), 6.95 (m, 3H), 5.62 (s, 1H), 3.84 (s, 3H), 3.32 (d, J = 12.1 Hz, 1H), 2.98 (d, J = 12.1 Hz, 1H). ^{13}C NMR (75.4 MHz, $DMSOd_6$) δ 168.4, 159.0, 136.4, 136.3, 130.3, 130.2, 128.5, 128.1, 127.5, 125.8, 114.2, 55.1, 45.6, 31.2. HRMS m/z (M + H)$^+$ calcd. for $C_{16}H_{15}ClNO_2S$ 320.0512, found 320.0504.

*7-Chloro-5-(2′-ethoxyphenyl)-3,5-dihydro-4,1-benzothiazepin-2-(1H)-one (**4g**).* Following the general procedure for the preparation of 7-chloro-5-aryl-3,5-dihydro-4,1-benzothiazepin-2-(1*H*)-ones **4a−j** and **1**, reaction of **3g** (100 mg, 0.27 mmol) with methyl thioglycolate (0.83 mmol, 88 mg) in TFA (3.98 mmol, 454 mg, 305 μL) yielded **4g** (57 mg, 65%) as a white solid. Mp 192−194 °C. ^{1}H NMR (200 MHz, $DMSOd_6$) δ 9.80 (m, 1H), 7.63 (d, J = 8.5, 1H), 7.34 (m, 2H), 7.04 (m, 3H), 6.78 (d, J = 2.4 Hz, 1H), 5.89 (s, 1H), 3.94 (m, 2H), 3.16 (d, J = 12.1 Hz, 1H), 2.96 (d, J = 12.1 Hz, 1H), 1.12 (t, J = 7.4 Hz, 3H). ^{13}C NMR (75.4 MHz, $DMSOd_6$) δ 168.6, 155.6, 136.6, 135.9, 130.2, 129.7, 129.6, 128.1, 127.2, 125.7, 124.9, 120.4, 112.7, 63.7, 31.0, 26.2, 14.4. HRMS m/z (M + H)$^+$ calcd. for $C_{15}H_{11}ClF_3N_2OS$ 334.0669, found 334.0677.

*7-Chloro-5-(4′-fluorophenyl)-3,5-dihydro-4,1-benzothiazepin-2-(1H)-one (**4h**).* Following the general procedure for the preparation of 7-chloro-5-aryl-3,5-dihydro-4,1-benzothiazepin-2-(1*H*)-ones **4a−j** and **1**, reaction of **3h** (315 mg, 0.90 mmol) with methyl thioglycolate (2.70 mmol, 286 mg) in TFA (12.58 mmol, 1.43 g, 0.96 mL) yielded **4h** (163 mg, 59%) as a white solid. Mp 252−254 °C. ^{1}H NMR (200 MHz, $DMSOd_6$) δ 9.65 (s, 1H), 7.57 (m, 2H), 7.43 (dd, J = 8.4, 2.4 Hz, 1H), 7.32 (m, 2H), 7.08 (d, J = 8.4 Hz, 1H), 6.96 (d, J = 2.4 Hz, 1H), 5.66 (s, 1H), 3.16 (d, J = 12.1 Hz, 1H), 2.99 (d, J = 12.1 Hz, 1H). ^{13}C NMR (75.4 MHz, $DMSOd_6$) δ 168.5, 164.2, 136.4 (d, J = 39.2 Hz), 133.7, 131.1 (d, J = 2.3 Hz), 130.4, 128.5, 127.9, 126.2, 115.9 (d, J = 6 Hz), 115.4, 45.8, 31.1. HRMS m/z (M + H)$^+$ calcd. for $C_{15}H_{12}ClFNOS$ 308.0312, found 308.0309.

*7-Chloro-5-(2′-bromophenyl)-3,5-dihydro-4,1-benzothiazepin-2-(1H)-one (**4i**).* Following the general procedure for the preparation of 7-chloro-5-aryl-3,5-dihydro-4,1-benzothiazepin-2-(1*H*)-ones **4a−j** and **1**, reaction of **3i** (292 mg, 0.71 mmol) with methyl thioglycolate (4.25 mmol, 451 mg) in TFA (9.92 mmol, 1.13 g, 760 μL) yielded **4i** (122 mg, 46%) as a white solid. Mp 204−206 °C. ^{1}H NMR (300 MHz, $CDCl_3$) δ 7.82 (m, 1H), 7.63 (d, J = 8.6 Hz, 1H), 7.47 (m, 1H), 7.27 (m, 2H), 7.10 (bs, 1H), 7.04 (d, J = 8.6 Hz, 1H), 6.69 (d, J = 1.8 Hz, 1H), 6.12 (s, 1H), 3.33 (d, J = 12.0 Hz, 1H), 3.03 (d, J = 12.0 Hz, 1H). ^{13}C NMR (50.2 MHz, $DMSOd_6$) δ 168.3, 136.7, 135.5, 134.4, 133.6, 131.1, 130.6, 130.5, 128.6, 128.4, 126.6, 125.8, 124.0, 45.6, 31.1. Anal. Calcd for $C_{15}H_{11}BrClNOS$: C, 48.87; H, 3.01; N, 3.80. Found: C, 48.49; H, 3.24; N, 3.69.

*7-Chloro-5-(2′,6′-dichlorophenyl)-3,5-dihydro-4,1-benzothiazepin-2-(1H)-one (**4j**).* Following the general procedure for the preparation of 7-chloro-5-aryl-3,5-dihydro-4,1-benzothiazepin-2-(1*H*)-ones **4a−j** and **1**, reaction of **3j** (325 mg, 0.81 mmol) with methyl thioglycolate (4.84 mmol, 514 mg) in TFA (11.30 mmol, 1.29 g, 865 μL) yielded **4j** (191 mg, 66%) as a white solid. Mp 208−211 °C. ^{1}H NMR (300 MHz, $CDCl_3$) δ 8.50 (bs, 1H), 7.43 (d, J = 8.6 Hz, 2H), 7.30−7.25 (m, 2H + residual $CHCl_3$), 7.05 (d, J = 9.0 Hz, 1H), 7.01 (s, 1H), 6.71 (s, 1H), 3.65 (d, J = 12.0 Hz, 1H), 3.05 (d, J = 12.0 Hz, 1H). ^{13}C NMR (75.4 MHz, $CDCl_3$) δ 170.9, 137.2, 135.6, 132.4, 131.3, 130.3, 130.2, 129.8, 129.7, 129.1, 125.5, 42.9, 32.0. Anal. Calcd for $C_{15}H_{10}Cl_3NOS$: C, 50.23; H, 2.81; N, 3.91. Found: C, 50.64; H, 2.51; N, 3.57.

*7-Chloro-5-(2′-chlorophenyl)-3,5-dihydro-4,1-benzothiazepin-2-(1H)-one (**1**).* Following the general procedure for the preparation of 7-chloro-5-aryl-3,5-dihydro-4,1-benzothiazepin-2-(1*H*)-ones **4a−j** and **1**, reaction of **3j** (311 mg, 0.93 mmol) with methyl thioglycolate (2.79 mmol, 296 mg) in TFA (13.38 mmol, 1.53 g, 1.03 mL) yielded **1** (174 mg, 65%) as a white solid, showing analytical and spectral data in accordance with the literature.[9]

Materials. None of the tested compounds present structural similarities with Pan Assay Interference Compounds (PAINS), according to the classification reported by Baell and Holloway.[47] Experiments using brains of Sprague−Dawley rats were conducted under European Union Council Directives and approved by the Biomedical Research Ethics Committee of the School of Medicine, UAM, Spain. Efforts to reduce the quantity of sacrificed animals and their suffering were made.

Measurements of Histamine-Induced $[Ca^{2+}]_m$ Oscillations and with Permeabilized HeLa Cells, in the Presence of Testing Compounds. HeLa cells were seeded and transfected with a low affinity to Ca^{2+} mitochondrial-targeted aequorin, a bioluminiscent Ca^{2+} sensitive probe. After 48 h of expression, cells were incubated for 1.5 h with its prosthetic group, native celenterazine (2.5 μM). Ca^{2+}-induced bioluminiscence was registered by a purposed-built luminometer. Photons were calibrated in terms of mitochondrial Ca^{2+} concentration ($[Ca^{2+}]_m$) by lysing cells with digitonin (100 μM) and by using a very high concentration of Ca^{2+} (up to 10 mM) at the end of every experiment in order to irreversibly quench the total functional aequorin, as described before.[48] The monolayer of cells expressing the mitochondrial aequorin was superfused during the whole experiment with extracellular Krebs-HEPES solution containing (in mM): 125 NaCl, 5 KCl, 1 Na_3PO_4, 1 $MgSO_4$, 5.5 glucose, 20 HEPES, 1 Ca^{2+}, with pH 7.4 at room temperature (24 ± 2 °C). For the experiments with histamine, a 30 s pulse of histamine (100 μM) was administered. For the direct measurement of mNCX activity using permeabilized HeLa cells, after luminiscence signal reached a steady level, cells were permeabilized for 15 s with 100 μM digitonin in an intracellular solution containing (in mM): 130 KCl, 10 NaCl, 1 K_3PO_4, 1 ATP, 5 sodium succinate, 10 HEPES, (pH 7 at 24 °C), supplemented with 0.5 mM EGTA. Then, cells were stabilized for 2 min with this intracellular solution, and then it was replaced by another solution containing 5 μM Ca^{2+} instead of EGTA. After Ca^{2+} entered into the mitochondrial matrix and reached a peak, to study the mitochondrial Ca^{2+} clearance, the solution was replaced by another containing compounds **1** or **4c** at different concentrations, or 0 Na^+ plus KCl 10 mM (0 Na^+).

MTT Assay. The health of cells was assessed by means of monitoring their mitochondrial activity, with regard to the ability of chemically reducing the colorimetric MTT, as described previously,[35] with slight modifications. SH-SY5Y cells were cultured in 48-well plates. In the case of using hippocampal slices, after Glu exposure, they were suspended into 48-well plates. MTT was applied (5 mg·mL^{-1}), and the chemical reduction was allowed to proceed in the dark at 37 °C for 2 h (30 min in the case of hippocampal slices). MTT possesses a tetrazolium ring, which is cleaved by mitochondrial hydrogenases, thus forming a formazan product that is precipitated in the buffer media. After harvesting the medium, formazan was dissolved with 300 μL of DMSO, generating a violet-color, whose intensity was measured

DOI: 10.1021/acschemneuro.5b00161
ACS Chem. Neurosci. 2015, 6, 1626−1636

in a colorimetric plate reader at the wavelength of 540 nm (FLUOstar Optima, BMG, Germany). Data were reported as percentage of chemical reduction of MTT compared to the value found in the control situation in absence of toxic stimuli, which was considered as 100% viability. Data are commented as the percentage of protection exerted by a compound. Thus, when a 50% decrease in MTT-derived absorbance is observed in control group (with toxic stimulus but absence of compounds), it means a 50% of loss of cell viability. Then, a decrease of 25% in such loss of cell viability in a test group (with toxic stimulus plus the presence of a tested compound), it means a 50% of neuroprotection.

Recording of Whole Cell Currents Through VGCCs. For patch-clamp recording of whole-cell Ca^{2+} currents (I_{Ca}), the perforated-patch mode of the patch-clamp technique was used,[49,50] using amphotericin B as the permeating agent in bovine chromaffin cells.[51,52] Tight seals (>5 GΩ) were achieved in a standard Tyrode solution composed of (in mM): 137 NaCl, 1 $MgCl_2$, 5 $CaCl_2$, 5.3 KCl, 10 glucose, and 10 HEPES; tetrodotoxin was added at 1 μM to block Na^+ currents. The intracellular solution had the following composition (in mM): 100 CsCl, 14 EGTA, 20 TEA-Cl, 10 NaCl, 5 Mg-ATP, 0.3 Na-GTP, and 20 HEPES/CsOH, pH 7.3. I_{Ca} values were recorded at room temperature (22−25 °C) using an EPC-10 patch-clamp amplifier (HEKA Elektronik, Lambrecht, Germany) controlled by PULSE software running on a personal computer. The access resistance was monitored until it decreased to <20 MΩ. In all recordings, the holding potential was −80 mV. I_{Ca}'s were activated in response to 50 ms depolarizing voltage steps from −80 to 0 mV. I_{Ca} amplitude was measured at the maximum peak current during the 50 ms depolarizing pulse. Test voltage protocol was applied every 15 s during the next 3 min, when a balance in the maximum degree of blocking was reached. Current signals were filtered at 5 kHz, digitized at 50 kHz, and online leak subtracted via a P/4 protocol.

Data Analysis. Data are presented as means ± SEM. Peak increases of the $[Ca^{2+}]_m$ elevations and areas under the curve (AUC) were determined by using Origin 5.0 (OriginLab Corporation, Northampton, MA). Statistical differences were assessed by ANOVA followed by Newman−Keuls post hoc analysis. Statistical differences were taken as significant when $p \leq 0.05$. All statistical analyses were performed using Prism software (GraphPad) version 5.0 for Mac (OS X).

■ ASSOCIATED CONTENT

Supporting Information

^1H and ^{13}C NMR spectra of compounds **4d−j**, cell and tissue culture protocols, LDH assay protocol, DCFDA experiment protocol, quantitative data of neuroprotection experiments, dose−response analysis of **1** on the $[Ca^{2+}]_m$ decay rate in histamine-stimulated HeLa cells, HeLa cell viability in the presence of **1** and **4c**, and DCFDA experiment in the presence of **1** and **4c**. The Supporting Information is available free of charge on the ACS Publications website at DOI: 10.1021/acschemneuro.5b00161.

■ AUTHOR INFORMATION

Corresponding Authors

*C.d.l.R.: phone, +34-914972765; fax, +34-914973453; e-mail, cristobal.delosrios@uam.es

*M.F.C.-A.: phone, +34-915202372; fax, +34-914973453; e-mail, maria.cano@uam.es.

Present Address

§J.C.F.-M.: Cardiac Signaling Center of University of South Carolina, Medical University of South Carolina and Clemson University, Charleston, SC, USA.

Author Contributions

F.J.M.-S. performed most of the chemical synthesis and the assessment of the mNCX blockade, R.L.-C. reviewed the manuscript, conducted chemical synthesis and the neuroprotection experiments in bovine chromaffin cells, A.J.M.-O. oversaw the experiments of mNCX blockade and performed the experiments of viability in HeLa cells, L.G.-L. conducted the pharmacological experiments in SH-SY5Y cells and hippocampal slices, J.C.F.-M. performed the patch-clamp experiments, R.L.-A. synthesized compounds **3j** and **4j**, M.F.C.-A. conceived, designed, and oversaw all the pharmacological experiments in HeLa cells, and C.d.l.R. oversaw chemical synthesis and the pharmacological experiments in SH-SY5Y cells, hippocampal slices, and bovine chromafffin cells, and wrote the paper.

Funding

This work was supported by the following grants: Programa Miguel Servet (CP10/00531, IS Carlos III), Proyectos de Investigación en Salud (PI13/00789, IS Carlos III), and Ayuda Red CIEN (PI016/09, IS Carlos III). A.J.M.-O. is granted by Ministry of Economy (FPU program, ref AP2009/0343). R.L.-C is granted by Universidad Autónoma de Madrid. We thank the continued support of Fundación de Investigación Biomédica, Hospital Universitario de la Princesa, and Fundación Teófilo Hernando.

Notes

The authors declare no competing financial interest.

■ ABBREVIATIONS

AD, Alzheimer's disease; EC_{50}, half-maximal effective concentration; EGTA, ethylene glycol tetraacetic acid; ER, endoplasmic reticulum; Glu, glutamate; HEPES, (4-(2-hydroxyethyl)-1-piperazineethanesulfonic acid); I_{Ca}, Ca^{2+} currents; IP3, inositol triphosphate; LDH, lactate dehydrogenase; LiHMDS, lithium bis(trimethylsilyl)amide; mNCX, mitochondrial Na^+/Ca^{2+} exchanger; MTT, 3-(4,5-dimethylthiazol-2-yl)-2,5-diphenyltetrazolium bromide; NCLX, Na^+/Ca^{2+} or Li^+/Ca^{2+} exchanger; NMDA, *N*-methyl-D-aspartate; R/O, rotenone plus oligomycin A; SEM, standard error of the mean; SERCA, sarcoendoplasmic reticulum Ca^{2+} ATP-ase; TFA, trifluoroacetic acid; TTX, tetrodotoxin; VGCC, voltage-gated Ca^{2+} channels

■ REFERENCES

(1) Carafoli, E. (2012) The interplay of mitochondria with calcium: an historical appraisal. *Cell Calcium 52*, 1−8.

(2) Montero, M., Alonso, M. T., Carnicero, E., Cuchillo-Ibanez, I., Albillos, A., Garcia, A. G., Garcia-Sancho, J., and Alvarez, J. (2000) Chromaffin-cell stimulation triggers fast millimolar mitochondrial Ca2+ transients that modulate secretion. *Nat. Cell Biol. 2*, 57−61.

(3) De Stefani, D., Raffaello, A., Teardo, E., Szabo, I., and Rizzuto, R. (2011) A forty-kilodalton protein of the inner membrane is the mitochondrial calcium uniporter. *Nature 476*, 336−340.

(4) Palty, R., Silverman, W. F., Hershfinkel, M., Caporale, T., Sensi, S. L., Parnis, J., Nolte, C., Fishman, D., Shoshan-Barmatz, V., Herrmann, S., Khananshvili, D., and Sekler, I. (2010) NCLX is an essential component of mitochondrial Na+/Ca2+ exchange. *Proc. Natl. Acad. Sci. U. S. A. 107*, 436−441.

(5) Giacomello, M., Drago, I., Pizzo, P., and Pozzan, T. (2007) Mitochondrial Ca2+ as a key regulator of cell life and death. *Cell Death Differ. 14*, 1267−1274.

(6) Szabadkai, G., Simoni, A. M., Bianchi, K., De Stefani, D., Leo, S., Wieckowski, M. R., and Rizzuto, R. (2006) Mitochondrial dynamics and Ca2+ signaling. *Biochim. Biophys. Acta, Mol. Cell Res. 1763*, 442−449.

(7) Palty, R., Hershfinkel, M., and Sekler, I. (2012) Molecular identity and functional properties of the mitochondrial Na+/Ca2+ exchanger. *J. Biol. Chem. 287*, 31650−31657.

DOI: 10.1021/acschemneuro.5b00161
ACS Chem. Neurosci. 2015, 6, 1626−1636

(8) Boyman, L., Williams, G. S., Khananshvili, D., Sekler, I., and Lederer, W. J. (2013) NCLX: the mitochondrial sodium calcium exchanger. *J. Mol. Cell. Cardiol. 59*, 205−213.
(9) Pei, Y., Lilly, M. J., Owen, D. J., D'Souza, L. J., Tang, X. Q., Yu, J., Nazarbaghi, R., Hunter, A., Anderson, C. M., Glasco, S., Ede, N. J., James, I. W., Maitra, U., Chandrasekaran, S., Moos, W. H., and Ghosh, S. S. (2003) Efficient syntheses of benzothiazepines as antagonists for the mitochondrial sodium-calcium exchanger: potential therapeutics for type II diabetes. *J. Org. Chem. 68*, 92−103.
(10) Lee, B., Miles, P. D., Vargas, L., Luan, P., Glasco, S., Kushnareva, Y., Kornbrust, E. S., Grako, K. A., Wollheim, C. B., Maechler, P., Olefsky, J. M., and Anderson, C. M. (2003) Inhibition of mitochondrial Na+-Ca2+ exchanger increases mitochondrial metabolism and potentiates glucose-stimulated insulin secretion in rat pancreatic islets. *Diabetes 52*, 965−973.
(11) Castaldo, P., Cataldi, M., Magi, S., Lariccia, V., Arcangeli, S., and Amoroso, S. (2009) Role of the mitochondrial sodium/calcium exchanger in neuronal physiology and in the pathogenesis of neurological diseases. *Prog. Neurobiol. 87*, 58−79.
(12) Vaghy, P. L., Johnson, J. D., Matlib, M. A., Wang, T., and Schwartz, A. (1982) Selective inhibition of Na^+-induced Ca^{2+} release from heart mitochondria by diltiazem and certain other Ca^{2+} antagonist drugs. *J. Biol. Chem. 257*, 6000−6002.
(13) Chiesi, M., Schwaller, R., and Eichenberger, K. (1988) Structural dependency of the inhibitory action of benzodiazepines and related compounds on the mitochondrial Na+-Ca2+ exchanger. *Biochem. Pharmacol. 37*, 4399−4403.
(14) Gonzalez-Lafuente, L., Egea, J., Leon, R., Martinez-Sanz, F. J., Monjas, L., Perez, C., Merino, C., Garcia-De Diego, A. M., Rodriguez-Franco, M. I., Garcia, A. G., Villarroya, M., Lopez, M. G., and de Los Rios, C. (2012) Benzothiazepine CGP37157 and its isosteric 2′-methyl analogue provide neuroprotection and block cell calcium entry. *ACS Chem. Neurosci. 3*, 519−529.
(15) Baron, K. T., and Thayer, S. A. (1997) CGP37157 modulates mitochondrial Ca2+ homeostasis in cultured rat dorsal root ganglion neurons. *Eur. J. Pharmacol. 340*, 295−300.
(16) Czyz, A., and Kiedrowski, L. (2003) Inhibition of plasmalemmal Na(+)/Ca(2+) exchange by mitochondrial Na(+)/Ca(2+) exchange inhibitor 7-chloro-5-(2-chlorophenyl)-1,5-dihydro-4,1-benzothiazepin-2(3H)-one (CGP-37157) in cerebellar granule cells. *Biochem. Pharmacol. 66*, 2409−2411.
(17) Nicolau, S. M., de Diego, A. M., Cortes, L., Egea, J., Gonzalez, J. C., Mosquera, M., Lopez, M. G., Hernandez-Guijo, J. M., and Garcia, A. G. (2009) Mitochondrial Na+/Ca2+-exchanger blocker CGP37157 protects against chromaffin cell death elicited by veratridine. *J. Pharmacol. Exp. Ther. 330*, 844−854.
(18) Tu, S. J., Cao, X. D., Hao, W. J., Zhang, X. H., Yan, S., Wu, S. S., Han, Z. G., and Shi, F. (2009) An efficient and chemoselective synthesis of benzo[e][1,4]thiazepin-2(1H,3H,5H)-ones via a microwave-assisted multi-component reaction in water. *Org. Biomol. Chem. 7*, 557−563.
(19) Ghorai, M. K., Sahoo, A. K., and Bhattacharyya, A. (2014) Syntheses of Imidazo-, Oxa-, and Thiazepine Ring Systems via Ring-Opening of Aziridines/Cu-Catalyzed C-N/C-C Bond Formation. *J. Org. Chem. 79*, 6468−6479.
(20) Bezprozvanny, I. (2009) Calcium signaling and neurodegenerative diseases. *Trends Mol. Med. 15*, 89−100.
(21) Murray, F. E., Landsberg, J. P., Williams, R. J., Esiri, M. M., and Watt, F. (1992) Elemental analysis of neurofibrillary tangles in Alzheimer's disease using proton-induced X-ray analysis. *Ciba Found. Symp. 169*, 201−210.
(22) Mark, R. J., Hensley, K., Butterfield, D. A., and Mattson, M. P. (1995) Amyloid beta-peptide impairs ion-motive ATPase activities: evidence for a role in loss of neuronal Ca^{2+} homeostasis and cell death. *J. Neurosci. 15*, 6239−6249.
(23) Danzer, K. M., Haasen, D., Karow, A. R., Moussaud, S., Habeck, M., Giese, A., Kretzschmar, H., Hengerer, B., and Kostka, M. (2007) Different species of alpha-synuclein oligomers induce calcium influx and seeding. *J. Neurosci. 27*, 9220−9232.
(24) Guzman, J. N., Sanchez-Padilla, J., Wokosin, D., Kondapalli, J., Ilijic, E., Schumacker, P. T., and Surmeier, D. J. (2010) Oxidant stress evoked by pacemaking in dopaminergic neurons is attenuated by DJ-1. *Nature 468*, 696−700.
(25) Appel, S. H., Beers, D., Siklos, L., Engelhardt, J. I., and Mosier, D. R. (2001) Calcium: the Darth Vader of ALS. *Amyotrophic Lateral Scler. 2* (Suppl 1), 47−54.
(26) Tang, T. S., Tu, H., Chan, E. Y., Maximov, A., Wang, Z., Wellington, C. L., Hayden, M. R., and Bezprozvanny, I. (2003) Huntingtin and huntingtin-associated protein 1 influence neuronal calcium signaling mediated by inositol-(1,4,5) triphosphate receptor type 1. *Neuron 39*, 227−239.
(27) Zeron, M. M., Hansson, O., Chen, N., Wellington, C. L., Leavitt, B. R., Brundin, P., Hayden, M. R., and Raymond, L. A. (2002) Increased sensitivity to N-methyl-D-aspartate receptor-mediated excitotoxicity in a mouse model of Huntington's disease. *Neuron 33*, 849−860.
(28) Fillit, H. M., Smith Doody, R., Binaso, K., Crooks, G. M., Ferris, S. H., Farlow, M. R., Leifer, B., Mills, C., Minkoff, N., Orland, B., Reichman, W. E., and Salloway, S. (2006) Recommendations for best practices in the treatment of Alzheimer's disease in managed care. *Am. J. Geriatr. Pharmacother. 4* (Suppl. A), S9−S24 quiz S25−S28.
(29) Blasco, H., Mavel, S., Corcia, P., and Gordon, P. H. (2014) The glutamate hypothesis in ALS: pathophysiology and drug development. *Curr. Med. Chem. 21*, 3551−3575.
(30) Kang, S., Cooper, G., Dunne, S. F., Dusel, B., Luan, C. H., Surmeier, D. J., and Silverman, R. B. (2012) CaV1.3-selective L-type calcium channel antagonists as potential new therapeutics for Parkinson's disease. *Nat. Commun. 3*, 1146.
(31) Dreses-Werringloer, U., Lambert, J. C., Vingtdeux, V., Zhao, H., Vais, H., Siebert, A., Jain, A., Koppel, J., Rovelet-Lecrux, A., Hannequin, D., Pasquier, F., Galimberti, D., Scarpini, E., Mann, D., Lendon, C., Campion, D., Amouyel, P., Davies, P., Foskett, J. K., Campagne, F., and Marambaud, P. (2008) A polymorphism in CALHM1 influences Ca2+ homeostasis, Abeta levels, and Alzheimer's disease risk. *Cell 133*, 1149−1161.
(32) Moreno-Ortega, A. J., Martinez-Sanz, F. J., Lajarin-Cuesta, R., de Los Rios, C., and Cano-Abad, M. F. (2015) Benzothiazepine CGP37157 and its 2′-isopropyl analogue modulate Ca(2+) entry through CALHM1. *Neuropharmacology 95*, 503−510.
(33) El Alaoui, A., Schmidt, F., Sarr, M., Decaudin, D., Florent, J. C., and Johannes, L. (2008) Synthesis and properties of a mitochondrial peripheral benzodiazepine receptor conjugate. *ChemMedChem 3*, 1687−1695.
(34) Ota, M., Narahashi, T., and Keeler, R. F. (1973) Effects of veratrum alkaloids on membrane potential and conductance of squid and crayfish giant axons. *J. Pharmacol. Exp. Ther. 184*, 143−154.
(35) Denizot, F., and Lang, R. (1986) Rapid colorimetric assay for cell growth and survival. Modifications to the tetrazolium dye procedure giving improved sensitivity and reliability. *J. Immunol. Methods 89*, 271−277.
(36) Rabkin, S. W., and Kong, J. Y. (2000) Nifedipine does not induce but rather prevents apoptosis in cardiomyocytes. *Eur. J. Pharmacol. 388*, 209−217.
(37) Choi, D. W. (1988) Glutamate neurotoxicity and diseases of the nervous system. *Neuron 1*, 623−634.
(38) Abramov, A. Y., and Duchen, M. R. (2010) Impaired mitochondrial bioenergetics determines glutamate-induced delayed calcium deregulation in neurons. *Biochim. Biophys. Acta, Gen. Subj. 1800*, 297−304.
(39) Bonda, D. J., Wang, X., Perry, G., Nunomura, A., Tabaton, M., Zhu, X., and Smith, M. A. (2010) Oxidative stress in Alzheimer disease: a possibility for prevention. *Neuropharmacology 59*, 290−294.
(40) Radi, E., Formichi, P., Battisti, C., and Federico, A. (2014) Apoptosis and Oxidative Stress in Neurodegenerative Diseases. *J. Alzheimer's Dis.*, DOI: 10.3233/JAD-132738.
(41) Egea, J., Rosa, A. O., Cuadrado, A., Garcia, A. G., and Lopez, M. G. (2007) Nicotinic receptor activation by epibatidine induces heme

DOI: 10.1021/acschemneuro.5b00161
ACS Chem. Neurosci. 2015, 6, 1626−1636

oxygenase-1 and protects chromaffin cells against oxidative stress. *J. Neurochem. 102*, 1842−1852.
(42) Romero, A., Egea, J., Garcia, A. G., and Lopez, M. G. (2010) Synergistic neuroprotective effect of combined low concentrations of galantamine and melatonin against oxidative stress in SH-SY5Y neuroblastoma cells. *J. Pineal Res. 49*, 141−148.
(43) Filippin, L., Magalhaes, P. J., Di Benedetto, G., Colella, M., and Pozzan, T. (2003) Stable interactions between mitochondria and endoplasmic reticulum allow rapid accumulation of calcium in a subpopulation of mitochondria. *J. Biol. Chem. 278*, 39224−39234.
(44) Hernandez-SanMiguel, E., Vay, L., Santo-Domingo, J., Lobaton, C. D., Moreno, A., Montero, M., and Alvarez, J. (2006) The mitochondrial Na+/Ca2+ exchanger plays a key role in the control of cytosolic Ca2+ oscillations. *Cell Calcium 40*, 53−61.
(45) Yamaguchi, I., Ikezawa, K., Takada, T., and Kiyomoto, A. (1974) Studies on a new 1,5-benzothiazepine derivative (CRD-401) VI. Effects on renal blood flow and renal function. *Jpn. J. Pharmacol. 24*, 511−522.
(46) Ragone, M. I., Torres, N. S., and Consolini, A. E. (2013) Energetic study of cardioplegic hearts under ischaemia/reperfusion and [Ca(2+)] changes in cardiomyocytes of guinea-pig: mitochondrial role. *Acta Physiol. 207*, 369−384.
(47) Baell, J. B., and Holloway, G. A. (2010) New substructure filters for removal of pan assay interference compounds (PAINS) from screening libraries and for their exclusion in bioassays. *J. Med. Chem. 53*, 2719−2740.
(48) Rizzuto, R., Simpson, A. W., Brini, M., and Pozzan, T. (1992) Rapid changes of mitochondrial Ca2+ revealed by specifically targeted recombinant aequorin. *Nature 358*, 325−327.
(49) Lindau, M., and Fernandez, J. M. (1986) A patch-clamp study of histamine-secreting cells. *J. Gen. Physiol. 88*, 349−368.
(50) Horn, R., and Marty, A. (1988) Muscarinic activation of ionic currents measured by a new whole-cell recording method. *J. Gen. Physiol. 92*, 145−159.
(51) Aggett, P. J., Fenwick, P. K., and Kirk, H. (1982) The effect of amphotericin B on the permeability of lipid bilayers to divalent trace metals. *Biochim. Biophys. Acta, Biomembr. 684*, 291−294.
(52) Rae, J., Cooper, K., Gates, P., and Watsky, M. (1991) Low access resistance perforated patch recordings using amphotericin B. *J. Neurosci. Methods 37*, 15−26.

DOI: 10.1021/acschemneuro.5b00161
ACS Chem. Neurosci. 2015, 6, 1626−1636